Diagnosis of the AC Current Densities Effect on the Cathodic Protection Performance of the Steel X70 for a Buried Pipeline due to Electromagnetic Interference Caused by HVPTL

M'hamed Ouadah[1, 2, *], Omar Touhami[1], and Rachid Ibtiouen[1]

Abstract—This paper diagnoses the effect of the AC current densities induced by the electromagnetic interferences between high voltage power line and buried power line on the cathodic protection performances of the X70 steel in the simulated soil. First, the induced voltage onto the pipeline was calculated for various power line configurations, separation distances between transmission line and pipeline and parallelism lengths. The induced AC current density was computed function to the induced voltage, soil resistivity, and holiday diameter. Then, the electrochemical characters of the X70 steel, at various AC current densities, are measured using the potentiodynamic method. The electrochemical parameters obtained by the electrochemical tests are used as boundary conditions in the cathodic protection simulation model. The results indicate that, under influence of AC current densities, the X70 steel is more susceptible to corrosion, and the cathodic protection is unable to maintain the protection potential.

1. INTRODUCTION

With the rapid development of the world economy, the demand for energy and transportation is also increasing rapidly. For this reason, it is necessary to build more high voltage power transmission lines (HVPTL) and oil or gas pipelines. Due to various factors, more and more oil/gas pipeline routes are in parallel with or crosses high voltage power transmission lines. An electric energy is transferred from high voltage power line to the pipeline. Its transfer to the metallic pipeline can be achieved by three possible mechanisms: the capacitive coupling, resistive or conductive coupling, and electromagnetic or inductive coupling [1–8].

The electromagnetic induction is the primary interference effect of high voltage power line on a buried pipeline during normal operation. This effect is similar to the coupling in a transformer, with the high voltage line acting as the primary coil, and the pipeline as the secondary coil. Electromagnetic induction occurs when alternating current flowing power line conductors generate an electromagnetic field around the conductors, which can couple with adjacent buried pipelines, inducing a voltage and current on the structure. The voltages and currents can be induced on the pipelines, from HVPTL, in the areas where they run in parallel and together. The level of induced voltage from an HVPTL on an adjacent pipeline is function of geometry, distance between the power line and pipeline, and the parallelism between power line and pipeline. The induced AC currents are function of induced voltage, soil resistivity, and coating defect diameter. These induced voltages and currents may be dangerous for the pipeline due to corrosive effects (AC corrosion) and cathodic protection installations [9–18].

Several researchers studied the effect of the AC current densities on the cathodic protection effectiveness [19, 20]. Xu et al. [20] experimentally studied the effects of alternating current density

---

on the performances of cathodic protection. They found that the presence of AC current density decreased the cathodic protection effectiveness to protect the steel from corrosion.

In this paper, in addition to study of the factors affecting the electromagnetic interference between high voltage power line and buried pipeline, we added to the previous works the effect of the AC current densities on the cathodic protection of the X70 steel pipelines. In this object, the electrochemical characters of the X70 steel with and without influence of the AC current densities are measured using the potentiodynamic method. The electrochemical corrosion parameters including corrosion potential, corrosion current density and Tafel slope are obtained from the polarization curves. These electrochemical parameters are used as boundary conditions in the cathodic protection simulation model. The results show that the superposed AC current density accelerates the corrosion degree of X70 steel in simulated soil solution by comparison with that in the absence of the AC density. The presence of AC current densities reduces the effectiveness of the cathodic protection.

2. INDUCED VOLTAGES AND AC CURRENT DENSITIES

The induced voltage (V_{pipe}) on the pipeline is generated by the electromagnetic field in the soil. The level of induced voltage from a high voltage power transmission line on an adjacent pipeline is a function of HVPTL parameters and of the mutual impedance between phase conductors of HVPTL and pipeline.

$$V_{pipe} = \sum_{i=1}^{3} Z_{PH(i)-P} I_i \tag{1}$$

where V_{pipe} is the induced voltage on the pipeline due to full load currents and $Z_{PH(i)-P}$ the mutual impedance with earth return between the ith-phase conductor of HVPTL and pipeline. The mutual impedance can be calculated as follows [21, 22]:

$$Z_{PH(i)-P} = \left(\mu_0 \cdot \frac{\omega}{8} \right) + j \left(\left(\mu_0 \cdot \frac{\omega}{2\pi} \right) \cdot \ln \left(\frac{1.85/\sqrt{\omega \cdot (\mu_0/\rho_{soil})}}{D_{PH(i)-P}} \right) \right) \tag{2}$$

where ρ_{soil} is the soil resistivity, μ_0 the space permeability, ω the angular frequency and $D_{PH(i)-P}$ the distance between phase conductor (i) and pipeline.

The induced AC current density (J_{AC}) at a circular holiday is a function of the induced voltage on pipeline (V_{pipe}), soil resistivity (ρ_{soil}), and holiday diameter (d). It can be computed as follows:

$$J_{AC} = \frac{8 \cdot V_{pipe}}{\rho_{soil} \cdot \pi \cdot d} \tag{3}$$

3. RESULTS

In this work, the calculations are carried out on two configurations of HVPTL (horizontal and vertical) as shown in Figure 1. The power lines have the following characteristics: $P = 400\,\text{MW}$ under $\cos(\theta) = 0.85$ and $U = 220\,\text{KV}$. The parallelism length between high voltage power transmission line and pipeline is 5 Km.

3.1. Factors Affecting the Electromagnetic Interference

In this section, we will present the impact of some factors on electromagnetic interferences.

3.1.1. Power Line Configuration

For $100\,\Omega \cdot \text{m}$ soil resistivity, the resulting induced AC voltage corresponding to the horizontal and vertical configurations as shown in Figure 2. From this figure, it can be seen that in the center of the power line, the horizontal configuration gives a lower amplitude value, whereas, when we move laterally from the center, this is the vertical configuration that gives lower amplitude.
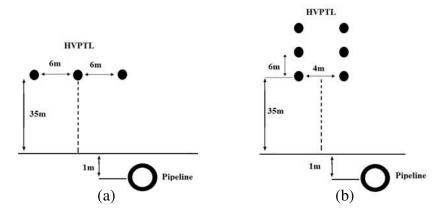
Figure 1. High voltage Power transmission line configuration. (a) Horizontal. (b) Vertical.
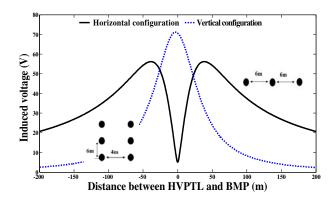

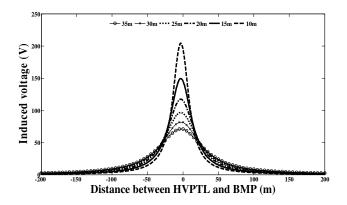**Figure 2.** Induced voltage for horizontal and vertical configurations.

Figure 3. Induced voltages at various heights for horizontal configuration.
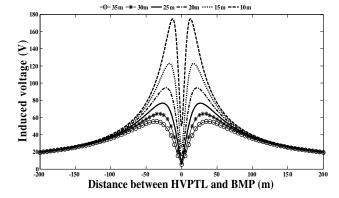

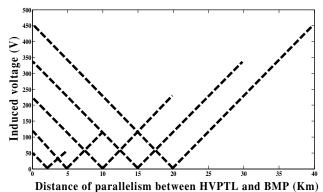**Figure 4.** Induced voltages at various heights for vertical configuration.

Figure 5. Induced voltage at various parallelism lengths.

3.1.2. High Distance between HVPTL and BMP

Figures 3 and 4 show the induced AC voltage at various heights (10 m, 15 m, 20 m, 25 m, 30 m and 35 m) of the HVPTL for horizontal and vertical configurations. From these figures, we can see that the increase in the distance between the pipeline and high voltage power line reduces the level of induced voltage on the pipeline. This can be explained by the fact that when the height of the power line increases, the electromagnetic field, seen by the pipeline decreases, causes a decrease in the amplitude of the induced voltage.

3.1.3. Parallelism between HVPTL and BMP

Figure 5 shows the induced voltage at various parallelism lengths between high voltage power line and pipeline (5 km, 10 km, 20 km, 30 km and 40 km). It is clearly seen that the magnitude of induced voltage on the pipeline is affected by the parallelism length. As the parallel length increases, the induced voltage on pipeline increases too.

3.2. Induced AC Current Densities

The current density varies linearly with induced voltage and depends on soil characteristics by its resistivity as it is shown in Figure 6. However, the current density increases with decreasing the dimension of the coating defect.

4. EFFECT OF AC CURRENT DENSITIES ON THE CATHODIC PROTECTION PERFORMANCE

The underground oil or gas pipelines are always protected against corrosion threats. Cathodic protection (CP) is a technique used to control the corrosion of a metal surface by making it the cathode of an electrochemical cell. There are two main CP system types: the sacrificial anode cathodic protection and the impressed current cathodic protection.

In order to study the influence of the AC current densities on cathodic protection effectiveness, a sacrificial anode cathodic protection model was simulated by finite element method. The basic elements of the cathodic protection system are: (1) the anode (r_1), (2) the cathode (r_2), and (3) the electrolyte (Ω). The design of CP system requires the solution of Laplace's equation $\nabla^2 \phi = 0$ with relevant boundary conditions to give the distribution of the potential and current density in the solution domain. Figure 7 shows different boundary conditions used according to the boundary nature.

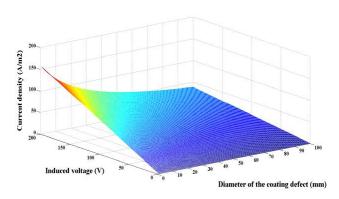For symmetry boundaries, the following boundary condition was used:

$$\frac{\partial \phi}{\partial n} = n \cdot \nabla \phi = 0 \tag{4}$$

where ϕ is the electrical potential and n the boundary surface normal.

For the anode and cathode surfaces, the boundary conditions used were as follows:

$$n \cdot J_a = -\sigma \frac{\partial \phi}{\partial n} = f_a(\phi) \tag{5}$$

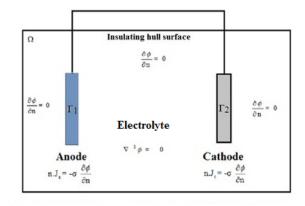$$n \cdot J_c = -\sigma \frac{\partial \phi}{\partial n} = f_c(\phi) \tag{6}$$

Figure 6. Induced current densities.

Figure 7. Principle of the cathodic protection system boundary conditions, Γ_1 is the anode, Γ_2 is the cathode and Ω is the electrolyte.

where J_a and J_c are the current densities at the anode and cathode, respectively, and σ is the electrolyte conductivity. $f_a(\phi)$ and $f_c(\phi)$ are functions that reflect the relationship between the current density and potential of the anode and cathode, respectively. The relationship between the current density and potential is generally described by a nonlinear curve, known as polarization curve obtained by electrochemical measurements.

The electrochemical measurements were performed using on a Bio-Logic SP-150 electrochemical workstation driven by a PC. The three-electrode system was used: X70 steel specimen was utilized as working electrode (WE). The geometric exposed area corresponding to the working electrode was $1\,\mathrm{cm}^2$. A saturated calomel electrode (SCE) has served as reference electrode (RE) and a platinum wire as counter electrode (CE). The AC current density was applied on the X70 electrode by two electrodes connected with the interference source, as shown in Figure 8. The electrolyte used in this study is the simulated soil solution. The chemical composition, PH and conductivity of the simulated soil solution are given in Table 1. All the experiments were accomplished at room temperature and under aeration conditions.

The polarization curves of X70 steel in simulated soil solution are obtained for scanning range between -1.6 and $0.2\,\mathrm{V\cdot SCE}$ using a scan rate of $1\,\mathrm{mV/s}$ from the cathode-anode direction. Figure 9 shows the polarization curves of X70 steel measured at an frequency of $50\,\mathrm{Hz}$ and various AC current densities ($0\,\mathrm{A/m}^2$, $100\,\mathrm{A/m}^2$ and $200\,\mathrm{A/m}^2$). In this figure, it can be seen that the polarization curves are different with an increase in the AC current density. Furthermore, the increase in the AC current density causes a positive shift of the corrosion potential and an increase in the corrosion current density. With an increase in the AC current density, the corrosion current density of the X70 steel increases. According to these results, we can conclude that the superposed AC current density accelerates the corrosion degree of X70 steel in simulated soil solution compared with that in the absence of the AC current density. The results of fitting the polarization curves from Figure 9 are summarized in Table 2, which shows the AC current density, corrosion potential (Ecorr), corrosion current density (Icorr) and Tafel slope (Ba, Bc).

Table 1. Simulated soil solution.

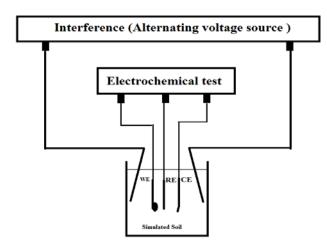| Composition	MgSO$_4$, 7H2O	CaCl$_2$, 2H$_2$O	KCl	NaCO$_3$
Weight (g)	0.131	0.18	0.122	0.483
PH		8.1		
T (°C)		23		

Figure 8. Alternating voltage source.

Figure 9. Polarization curves of the X70 steel in simulated soil at various AC current densities.

Table 2. Electrochemical parameters of X70 steel at various AC current densities.

AC (A/m^2)	Ecorr (mV·SCE)	Icorr (µA/cm^2)	Ba (mV)	Bc (mV)
0	−769.39	12.64	173.1	247.1
100	−731.39	31.41	175.5	466.3
200	−710.26	46.36	204.0	671.6

Figure 10. Model geometry.

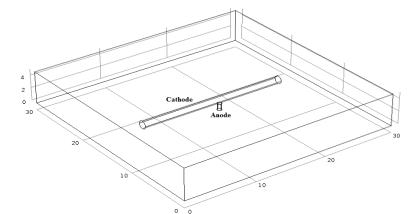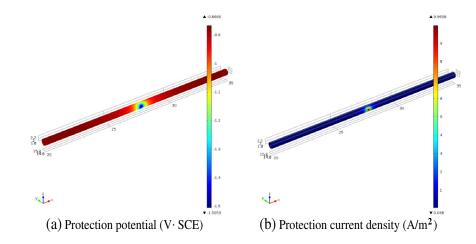(a) Protection potential (V·SCE)   (b) Protection current density (A/m^2)

Figure 11. (a) Contour plot of the protection potential, and (b) protection current density.

The model geometry of the cathodic protection system is a three-dimensional rectangular electrolyte volume with an anode and a cathode as shown in Figure 10. To introduce the AC current densities on the simulation model, the electrochemical parameters revealed by the polarization curves of the X70 steel in simulated soil solution at various AC current densities are used as boundary conditions at the cathode surface. At the anode surface, the potential of the sacrificial anode was assumed to be fixed. The boundary condition expresses that each point of the anode surface has the same potential. In this study, the potential of the sacrificial anode is −1.65 V.

Figure 11 shows the contours plot of the protection potential and the protection current density of the X70 steel pipeline without influence of the AC densities. The protection potential is in the range of −1.5053 V·SCE and −0.8666 V·SCE. We notice that the potential area facing the anode has the lowest value with −1.5053 V·SCE and increases with the location away from the anode. On the other hand,

(a) Protection potential (V· SCE) (b) Protection current density (A/m^2)

Figure 12. (a) Contour plot of the protection potential, and (b) protection current density for AC current density of 100 A/m^2.

(a) Protection potential (V· SCE) (b) Protection current density (A/m^2)

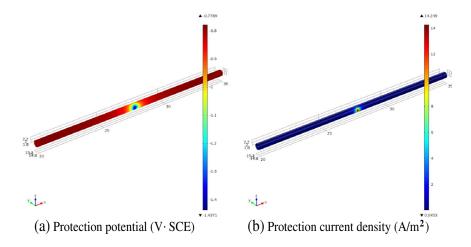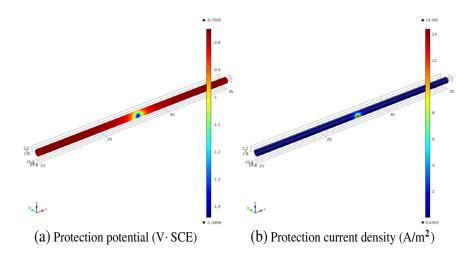**Figure 13.** (a) Contour plot of the protection potential, and (b) protection current density for AC current density of 200 A/m^2.
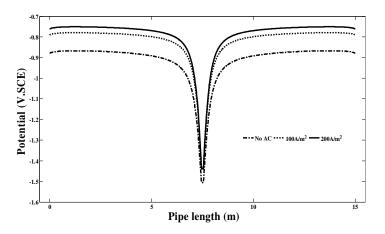

Figure 14. Protection potentials attenuation at various AC current densities.

the contour plot of the protection current density can clearly demonstrate that the current density area face to anode has the highest value $9.9658\,\mathrm{A/m^2}$ and decreases with the location away from the anode.

Figures 12 and 13 show the contours plot of the protection potential and protection current density on the X70 steel pipeline under the influence of AC density of $100\,\mathrm{A/m^2}$ and $200\,\mathrm{A/m^2}$, respectively. When the X70 steel pipeline is disturbed by the AC current densities, the protection potential of the X70 steel pipeline is altered, as shown in Figure 14. From the results, we notice that the increase in the AC current density causes a positive shift of the protection potential of the X70 steel pipeline and an increase in the protection current density. The cathodic protection is unable to maintain the protection potential in the presence of AC current densities. This means that the AC current density can cause AC corrosion of the steel pipelines even if there is a functioning cathodic protection system.

5. CONCLUSION

The most important conclusions reached by this study are as follows:

- As the parallel section increases, the induced voltage on pipeline increases too.
- The increase in the AC current density causes a positive shift of the corrosion potential and an increase in the corrosion current density.
- The X70 steel under AC current densities is more susceptible to corrosion in simulated soil solution.
- The cathodic protection is unable to maintain protection potential in the presence of AC current densities.

REFERENCES

1. Christoforidis, G. and D. Labridis, "Inductive Interference on pipelines buried in multilayer soil due to magnetic fields from nearby faulted power lines," *IEEE Transaction on Electromagnetic Compatibility*, Vol. 47, No. 2, 254–262, May 2005.
2. Gupta, A. and M. J. Thomas, "Coupling of high voltage AC power lines fields to metallic pipelines," *9th International Conference on Electro Magnetic Interference and Compatibility, INCEMIC*, Bangalore, India, February 23–24, 2006.
3. Saied, M. M., "The capacitive coupling between EHV lines and nearby pipelines," *IEEE Transactions on Power Delivery*, Vol. 19, No. 3, 1225–1231, 2004.
4. Braunstein, R., E. Schmautzer, and M. Oelz, "Impacts of inductive and conductive interference due to high-voltage lines on coating holidays of isolated metallic pipelines," *21st International Conference on Electricity Distribution*, 13, Frankfurt, Germany, June 2011.
5. Kopsidas, K. and I. Cotton, "Induced voltages on long aerial and buried pipelines due to transmission line transients," *IEEE Trans. Power Del.*, Vol. 23, No. 3, 1535–1543, July 2008.
6. Cotton, I., K. Kopsidas, and Y. Z. Elton, "Comparison of transient and power frequency-induced voltages on a pipeline parallel to an over-head transmission line," *IEEE Trans. Power Del.*, Vol. 22, No. 3, 1706–1714, July 2007.
7. Dawalibi, F. P. and R. D. Southey, "Analysis of electrical interference from power lines to gas pipelines, part II — Parametric analysis," *IEEE Trans. Power Del.*, Vol. 5, No. 1, 415–421, January 1990.
8. Hanafy, M. I., "Effect of oil pipelines existing in an HVTL corridor on the electric-field distribution," *IEEE Trans. Power Del.*, Vol. 22, No. 4, 2466–2471, 2007.
9. Zhang, R., P. R. Vairavanathan, and S. B. Lalvani, "Perturbation method analysis of AC-induced corrosion," *Corrosion Science*, Vol. 50, 1664–1671, 2008.
10. Goidanich, S., L. Lazzari, and M. Ormellese, "AC corrosion. Part 1: Effects on overpotentials of anodic and cathodic processes," *Corrosion Science*, Vol. 52, 491–497, 2010.
11. Goidanich, S., L. Lazzari, and M. Ormellese, "AC corrosion. Part 2: Parameters influencing corrosion rate," *Corrosion Science*, Vol. 52, 916–922, 2010.

12. Xu, L. Y., X. Su, Z. X. Yin, Y. H. Tang, and Y. F. Cheng, "Development of a real time AC/DC data acquisition technique for studies of AC corrosion of pipelines," *Corrosion Science*, Vol. 61, 215–223, 2012.

13. Nielsen, L. V. and F. Galsgaard, "Sensor technology for on-line monitoring of AC-induced corrosion along pipelines," *Corrosion'2005*, Paper No. 05375, NACE, Houston, USA.

14. Fu, A. Q. and Y. F. Cheng, "Effect of alternating current on corrosion and effectiveness of cathodic protection of pipelines," *Can. Metall. Q.*, 81–90, 2012.

15. Song, H. S., Y. G. Kim, S. M. Lee, and Y. T. Kho "Competition of AC and DC current in AC corrosion under cathodic protection" *Corrosion'2002*, Paper No. 02117, NACE, Houston, 2002.

16. Nielsen, L. V., "Role of alkalization in AC induced corrosion of pipelines and consequences hereof in relation to CP requirements," *Corrosion'2005*, Paper No. 05188, NACE, Houston, USA, 2005.

17. Xu, L. Y., X. Su, and Y. F. Cheng, "Effect of alternating current on cathodic protection on pipelines," *Corrosion Science*, Vol. 66, 263–268, 2013.

18. Ouadah, M., M. Zergoug, A. Ziouche, O. Touhami, R. Ibtiouen, S. Bouyegh, and C. Dehchar, "AC corrosion induced by high voltage power line on cathodically protected pipeline," *Proceedings Engineering & Technology (PET)*, Vol. 7, 2356–5608, 2014.

19. Nielsen, L. V., "Role of alkalization in AC induced corrosion of pipelines and consequences hereof in relation to CP requirements," *Corrosion'2005*, Paper No. 05188, NACE, Houston, USA, 2005.

20. Xu, L. Y., X. Su, and Y. F. Cheng, "Effect of alternating current on cathodic protection on pipelines," *Corrosion Science*, Vol. 66, 263–268, 2013.

21. Braunstein, R., E. Schmautzer, and G. Propst, "Comparison and discussion on potential mitigating measures regarding inductive interference of metallic pipelines," *Proceedings of ESARS*, Bologna, Italy, October 2010.

22. Hossam-Eldin, A., W. Mokhtar, and E. M. Ali, "Effect of electromagnetic fields from power lines on metallic objects and human bodies," *International Journal of Electromagnetic and Applications 2012*, Vol. 2, No. 6, 151–158, 2012.